PHYSICAL AND ORBITAL CHARACTERISTICS OF OBJECTS CONSTITUTING "SPACE JUNK" BASED ON DATA FROM OPTICAL GROUND-BASED OBSERVATIONS

Ognian Ognianov

Space Research and Technology Institute – Bulgarian Academy of Sciences
e-mail: ognianov@acceco.com

Keywords: *space debris, optical observations, astrometry, photometry, geostationary orbit (GEO), Space Surveillance and Tracking (SST)*

Abstract: *Optical ground-based telescopes are the main source of information on space debris in high orbits, where radar sensitivity falls with the fourth power of range. This paper reviews which orbital and physical characteristics of debris objects can be derived from optical data. Astrometry yields orbits, orbit-plane evolution in the geostationary region and area-to-mass ratios from solar radiation pressure perturbations. Photometry yields statistical size estimates, while light curves reveal rotation periods and attitude states. Colour indices and reflectance spectra give information on surface materials and their ageing. The methods are illustrated with observations of geostationary satellites and with orbit computations. Limitations, including the size–albedo degeneracy and the large number of uncorrelated detections, are discussed together with the role of optical sensors in the European SST network.*

ФИЗИЧЕСКИ И ОРБИТАЛНИ ХАРАКТЕРИСТИКИ НА ОБЕКТИТЕ, СЪСТАВЛЯВАЩИ „КОСМИЧЕСКИЯ БОКЛУК", ПО ДАННИ ОТ ОПТИЧНИ НАЗЕМНИ НАБЛЮДЕНИЯ

Огнян Огнянов

Институт за космически изследвания и технологии – Българска академия на науките
e-mail: ognianov@acceco.com

Ключови думи: *космически отломки, оптични наблюдения, астрометрия, фотометрия, геостационарна орбита (GEO), Космическо наблюдение и проследяване (SST)*

Резюме: *Оптичните наземни телескопи са основният източник на информация за космическите отломки във високи орбити, където чувствителността на радара пада с четвърта степен на обхвата. Тази статия разглежда кои орбитални и физически характеристики на обектите от отломки могат да бъдат извлечени от оптични данни. Астрометрията дава орбити, еволюция на орбитата-равнина в геостационарната област и съотношения площ-маса от смущения в налягането на слънчевата радиация. Фотометрията дава статистически оценки на размера, докато кривите на светлината разкриват периоди на въртене и състояния на положение. Цветните индекси и спектрите на отражение дават информация за повърхностните материали и тяхното стареене. Методите са илюстрирани с наблюдения на геостационарни спътници и с изчисления на орбити. Ограниченията, включително дегенерацията на размера и албедото и големият брой некорелирани засичания, са разгледани заедно с ролята на оптичните сензори в европейската мрежа на SST.*

1. Introduction

Space debris comprises all non-functional human-made objects in Earth orbit: defunct satellites, spent rocket bodies, mission-related objects and fragments from explosions and collisions. According to ESA, about 45,000 objects are regularly tracked by surveillance networks. Statistical models estimate about 54,000 objects larger than 10 cm, 1.2 million between 1 and 10 cm, and 140 million between 1 mm and 1 cm [11]. Kessler and Cour-Palais [1] showed that collisions can make such a population self-generating.

Radar dominates observations in low Earth orbit (LEO). Its echo power, however, decreases with the fourth power of range, whereas reflected sunlight decreases only with the square. Between 1,000 km and the geostationary orbit (GEO, about 36,000 km) the radar signal therefore drops by about six orders of magnitude, the optical signal by about three. Optical telescopes are thus the main tool for medium Earth orbit (MEO), geostationary transfer orbit (GTO), Molniya orbits and GEO [2].

This paper reviews which orbital and physical characteristics of debris can be derived from optical ground-based observations, and illustrates them with our own images and orbit computations.

2. Optical observations and data processing

2.1. Observing geometry. An object can be observed only when it is illuminated by the Sun while the observer is in darkness. For LEO this restricts observations to twilight; GEO objects are visible most of the night, except near the equinoxes, when they cross the Earth's shadow around local midnight. In long exposures, satellites appear as trails among the stars (Fig. 1).



Fig. 1. Milky Way with the trails of two aircraft and three satellites in a single exposure (photo: O. Ognianov)

2.2. Sensors. Representative optical facilities are ESA's 1 m Optical Ground Station (Space Debris Telescope) on Tenerife, the 0.61 m MODEST Schmidt telescope at Cerro Tololo [4], NASA's 1.3 m ES-MCAT on Ascension Island and the ISON network of small telescopes [5]. In Europe, the optical sensors complement a mostly radar-based network: GRAVES, TIRA, GESTRA, BIRALES and the EISCAT radars on the radar side; the Tenerife telescope, ZimLAT and ZimSMART in Zimmerwald and Starbrook on Cyprus on the optical side (Fig. 2). Meter-class telescopes reach magnitude 18–20, which corresponds to objects of about 10–25 cm in GEO (Section 4.1).

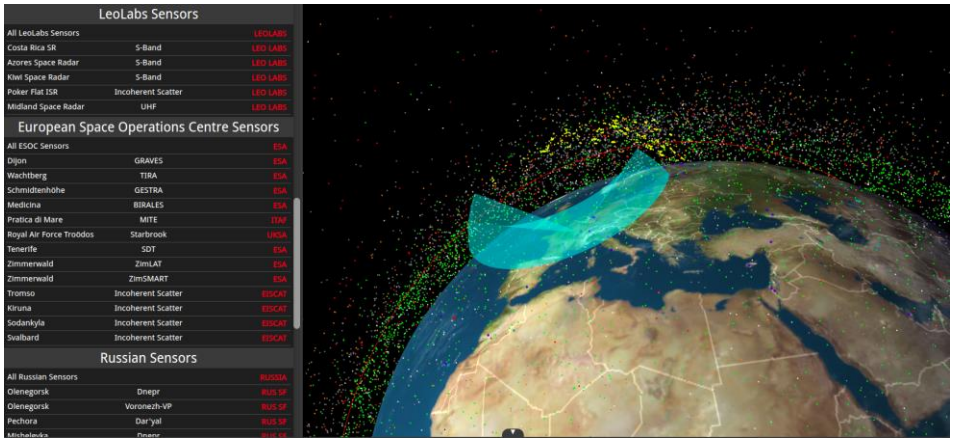


Fig. 2. European space observation centres and their sensors,
with the tracked population and a radar field of view over Europe (image: O. Ognianov)

2.3. Own observations. [Observing site(s), telescope aperture and focal length, camera, field of view, exposure times, observation period, number of frames and detected objects.]

2.4. Processing chain. The reduction of each night follows five steps:

1. Acquisition of CCD/CMOS frames in survey or follow-up mode.
1. Detection of streaks and point sources.
2. Astrometry: right ascension and declination of each object against reference stars (e.g. the Gaia catalogue).
3. Orbit determination: an initial orbit from a short arc, refined by a least-squares fit over several nights.
4. Correlation with the catalogue; an object without a match is classified as an uncorrelated target (UCT).

Fig. 3 shows a frame of the geostationary belt in which the satellites appear as short streaks. The objects were identified by comparing their measured positions with positions computed from catalogue orbits (Fig. 4).



Fig. 3. GEO satellites Express-AM7, Hellas Sat 2, Hellas Sat 3, PakSat-1R, Athena-Fidus and GOES 3 (image: O. Ognianov)

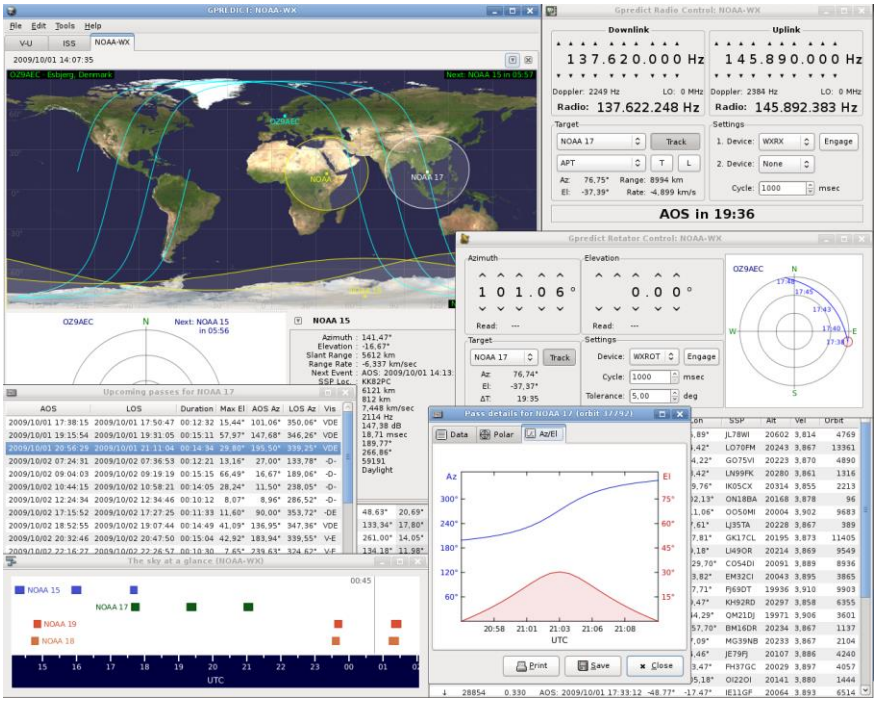


Fig. 4. Visualisation of calculated orbits: ground tracks, pass predictions and azimuth–elevation profiles in Gpredict (image: O. Ognianov)

3. Orbital characteristics

3.1. Distribution by orbital regime. The catalogued population forms a dense cloud in LEO and a distinct ring at geostationary altitude (Fig. 5). Optical surveys of the GEO ring show that a large share of faint detections cannot be correlated with any catalogued object [2, 3]; these uncorrelated targets are mostly small debris.

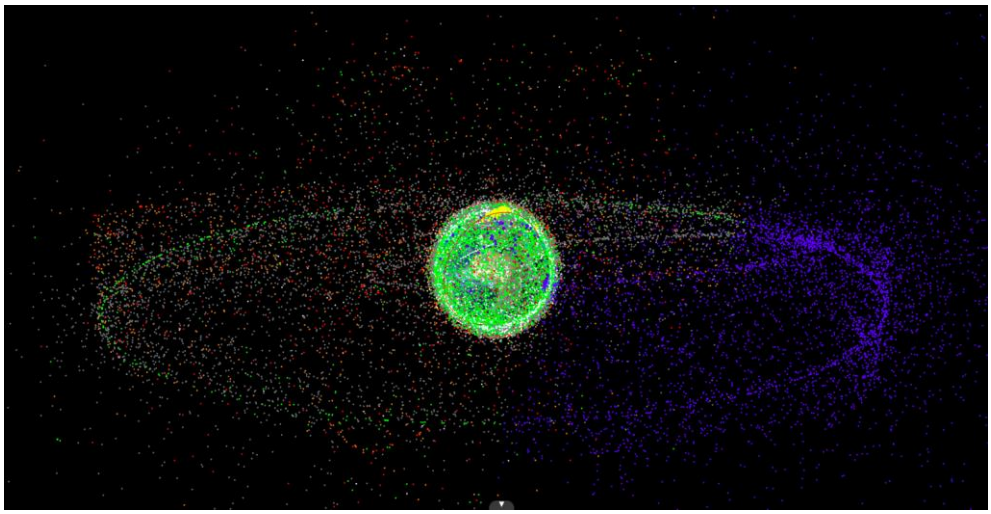


Fig. 5. Objects in Earth orbit: the dense LEO cloud and the GEO ring (image: O. Ognianov)

3.2. Orbit-plane evolution in GEO. Uncontrolled GEO objects are perturbed by the Sun, the Moon and the Earth's oblateness. Their orbital plane precesses around the Laplace plane, tilted by about 7.4° to the equator, with a period of about 53 years; the inclination oscillates between 0° and about 15° [2]. In the inclination-vector plane ($i\cdot\cos\Omega$, $i\cdot\sin\Omega$) these objects lie on a circle, which separates them clearly from station-kept satellites near the origin. In longitude, they either drift freely or librate around the stable points at 75° E and 105° W.

3.3. High area-to-mass-ratio objects. Surveys with the ESA telescope on Tenerife revealed faint objects in GEO-like orbits whose eccentricity changes quickly [3]. Their orbits can be fitted only with area-to-mass ratios (A/m) from about 1 to tens of m²/kg, compared with about 0.01–0.02 m²/kg for an intact satellite. They are most likely thin sheets such as multi-layer insulation. Solar radiation pressure drives a yearly oscillation of the eccentricity whose amplitude grows with A/m [6]; in a first-order model, the maximum eccentricity is about 0.03 per 1 m²/kg. Because their orbits change so fast, these objects are easily lost from the catalogue.

4. Physical characteristics

4.1. Size from brightness. For a diffusely reflecting (Lambertian) sphere of diameter d, albedo p and range R, the apparent magnitude is:

$$m = m_{\odot} \quad 2.5\log_{10}\left[\frac{2}{3}\,p\left(\frac{d}{2}\right)^{2}\frac{F(\varphi)}{R^{2}}\right],$$

where $m_{\odot} = -26.74$ is the magnitude of the Sun and $F(\varphi)$ is the phase function, normalised to $F(0) = 1$. Since the albedo of an individual object is unknown, a standard value $p = 0.175$ is commonly adopted [7]. Table 1 gives the resulting diameters in GEO.

Table 1. Diameter versus magnitude in GEO (R = 35,786 km, p = 0.175, φ = 0°)

Magnitude	Diameter (m)
14	1.5
16	0.6
18	0.24
20	0.09

An albedo anywhere between 0.05 and 0.4 changes the derived size by a factor of about 2.8, so sizes are meaningful statistically rather than for individual objects.

4.2. Rotation and attitude from light curves. Light curves show three main behaviours: a flat curve (stable or very slowly rotating objects), periodic variation with specular glints from flat surfaces such as solar panels, and aperiodic tumbling, typical of fragments [9]. The measured period is the apparent (synodic) period, which differs slightly from the sidereal spin period. Spin rates of defunct satellites change over years; Envisat, for example, rotated with a period of about two minutes in 2013, slowly lengthening [8].

4.3. Materials from colours and spectra. Colour indices (B–V, V–R, R–I) can be measured for faint objects, while reflectance spectra require brighter targets but show material features, such as the aluminium absorption near 830 nm [10]. Space weathering reddens and darkens surfaces over time, so spectra of old debris cannot be compared directly with laboratory spectra of fresh materials. The aim is to link material to origin, for example to distinguish multi-layer insulation fragments from paint flakes.

5. Discussion and conclusions

Optical ground-based observations provide the orbital picture of the debris population in MEO, GTO and GEO, together with physical properties that radar cannot easily obtain at these distances: area-to-mass ratios, statistical sizes, spin states and surface materials.

The main limitations are observing conditions (weather, Moon, night-time only), the degeneracy between size and albedo, and the large number of faint uncorrelated targets that are detected once and then lost. Satellite trails from large constellations increasingly contaminate survey images.

Future progress is expected from larger automated survey networks, machine-learning detection of streaks and combination with laser ranging and radar. These data calibrate debris environment models such as ESA MASTER and NASA ORDEM and support active debris removal missions, which need the spin state of a target before capture. Observers in Bulgaria can contribute to the European SST network through coordinated campaigns [12].

Acknowledgements

"Preparatory activities to join SSA program of ESA" (PASSA), Yavor Shopov, Penka Maglova, Alexey Stoev

References:

1. Kessler, D.J., Cour-Palais, B.G. (1978). Collision frequency of artificial satellites: the creation of a debris belt. J. Geophys. Res., 83(A6), 2637–2646.
6. Schildknecht, T. (2007). Optical surveys for space debris. Astron. Astrophys. Rev., 14, 41–111.
7. Schildknecht, T., et al. (2004). Optical observations of space debris in GEO and in highly-eccentric orbits. Adv. Space Res., 34, 901–911.
8. Seitzer, P., et al. (2004). MODEST observations of space debris at geosynchronous orbit. Adv. Space Res., 34, 1143–1149.
9. Molotov, I., et al. (2008). International scientific optical network for space debris research. Adv. Space Res., 41, 1022–1028.
10. Liou, J.-C., Weaver, J.K. (2005). Orbital dynamics of high area-to-mass ratio debris and their distribution in the geosynchronous region. Proc. 4th European Conference on Space Debris, ESA SP-587.
11. Mulrooney, M.K., Matney, M.J. (2007). Derivation and application of a global albedo yielding an optical brightness to physical size transformation free of systematic errors. Proc. AMOS Technical Conference.
12. Kucharski, D., et al. (2014). Attitude and spin period of space debris Envisat measured by satellite laser ranging. IEEE Trans. Geosci. Remote Sens., 52(12), 7651–7657.
13. Šilha, J., et al. (2018). Apparent rotation properties of space debris extracted from photometric measurements. Adv. Space Res., 61, 844–861.
14. Vananti, A., Schildknecht, T., Krag, H. (2017). Reflectance spectroscopy characterization of space debris. Adv. Space Res., 59, 2488–2500.
15. ESA Space Debris Office (2025). ESA's Space Environment Report 2025; Space Environment Statistics, sdup.esoc.esa.int/discosweb/statistics (accessed October 2026).
16. Ognyanov, O., Shopov, Y., Maglova, P., Stoev, A. Astrometry of artificial satellites based on cooperative observation campaigns. SES 2019.